Alternate bars growth and erosion under repeated hydrographs

Jingjing Xu,1 Dai Huang,1 and Toshiki Iwasaki 2

¹ Changjiang Institute of Survey, Planning, Design and Research Corporation, 430010 Wuhan, China; e-mail: daihuangdd@outlook.com;.Corresponding author.

² Faculty of Engineering, Hokkaido University, 0608628 Sapporo, Japan; e-mail: tiwasaki@eng.hokudai.ac.jp

ABSTRACT

The growth and erosion of alternate bars under unsteady flow conditions is an important topic in river morphodynamic, as alternate bars exhibit regular morphologies and similar sizes within the channel. This study employs a mathematical model to simulate the growth and erosion process of alternate bars under repeated hydrographs. The results reveal that the characteristics and evolution of alternate bars in unsteady flows demonstrates a strong time-dependence. With an appropriate cycle value, the variation of sandbars over time will reach a subtle consistency, but such phenomenon can't be reached if the cycle is too long or too short. We believe such phenomenon is caused since the response of alternate bars is not strong enough to destroy the original wavelength within a limited cycle, suggesting that the hydrograph cycle that achieves this equilibrium state must be moderately long such that the timescale of the hydrograph is similar but slightly smaller than the bar growth.

Keywords: alternate bars, unsteady discharge, morphodynamic equilibrium

1. Introduction

Understanding river morphology and its dynamics is an important topic in many research fields, and the alternate bar morphology is a specific field of interest. Owing to their spontaneous alternating transformation and migration, alternate bars could be the main contributing factor for channel engineering or watershed topography problems such as river bank protection, navigation, agriculture, or river construction. In the last few decades, extensive studies have investigated the fundamental physical mechanisms of the alternate bars. To understand river morphodynamics, the concept of formative (or dominant, effective) steady discharge, which determines the overall characteristics of river morphology, is adopted. River bars and related morphodynamics (e.g., meandering) have been thoroughly investigated using steady discharge conditions based on formative or effective discharge concepts. Generally, this simplification does not affect the fundamental physics of the formation and development of river bars and provides some important insights such as alternate bar wavelength and height, growth rate, and migration. Crosato et al. performed experiments and numerical simulations of alternate bar morphodynamics under long-term steady discharge conditions, demonstrating cyclic behavior of the alternate bar morphodynamics and the possibility of non-migrating alternate bars. However, these studies consider long-term dynamics of alternate bars to be in a relatively stable discharge condition.

On the other hand, the studies emphasize the significance of discharge unsteadiness on the morphodynamics of river bars always focus on short-term morphodynamics as only a single or

a few repeated hydrographs are considered. Instead, more longer-term behaviors of alternate bar dynamics need to be investigated in detail. In other words, exactly how the river bars were formed and continue to develop in the long term, under the complex sequence of hydrographs remains unclear. This is mainly owing to a lack of field observations pertaining to long-term interaction between hydrological events and spatiotemporal river bars, as well as the difficulty in performing long-term flume experiments, even under simplified conditions. Notably, in this regard, Carlin et al. proposed a novel framework for obtaining the long-term equilibrium characteristics of river bars (i.e., wavelength and wave height) using a linear, and nonlinear stability analysis with the flow duration curve, which is a simplified treatment of complex sequence of discharge variation in long-term. Their analyses agreed with field observations of the river bar geometry. This is a robust framework to understand the equilibrium state of bars under discharge variation; however, bar dynamics must be discussed in detail as discharge variations are simplified into a flow duration curve. Church and Rice investigated a centuryscale dynamics of point bars developed in a gravel-bed reach of lower Fraser River, British Columbia, Canada, showing response of bar dimension, namely, thickness, length, and width to the age of bars. Nelson and Morgan conducted flume experiments of gravel bedform development under repeated simple triangle hydrographs and a constant sediment feed rate. This is, to our knowledge, only the flume experiment to pursue long-term equilibrium of bedforms under unsteady discharge conditions. Their results showed that flow unsteadiness has a negligible effect on channel-scale morphologies. However, the bedform resembling the alternate bars in their experiment might be a combination of dunes and alternate bars (i.e., threedimensional bedforms, as the observed geometry does not satisfy the river bar categories derived from linear stability analysis that adopts the shallow flow approximation. In this case, the bedform can adjust its shape to the discharge variations, although there is a hysteresis effect. However, the large-scale bars have a longer morphodynamic timescale, so the effect of the hydrograph might be more complex. In summary, the discharge variation (or discharge unsteadiness) has been considered only recently in morphodynamic modeling, but it remains unclear how large-scale bedform alternate bars reach a state of equilibrium, especially in the long term.

This study focuses on the long-term behaviors of alternate bars under the influence of repeated hydrographs. To understand these points, we perform several numerical simulations of alternate bar formations under repeated hydrographs and corresponding steady discharge conditions using a two-dimensional morphodynamic model, iRIC-Nays2DH.

2. Method

2.1. Numerical model

We used the Nays2DH model, a two-dimensional morphodynamic model embedded in the iRIC software. This model was applied to various sediment transport-related simulation studies, and is suitable for simulating alternate bar morphodynamics focused on in this study. These model validations suggest that the Nays2DH model may be an acceptable tool to pursue the long-term morphodynamics of alternate bars under repeated hydrographs focused on in this study. Meanwhile, the flow model used is an unsteady two-dimensional shallow water flow model. As we focus on the morphodynamics of alternate bars in gravel-bed rivers, we only consider bedload transport as a mode of sediment transport. The Meyer-Peter and Müller

formula was used here, and the sediment was assumed to have a uniform grain size.

2.2 Computational conditions

We performed a straight modeled channel has a 21 km length and 70 m constant channel width with a uniform slope of 0.005. A Manning roughness coefficient of 0.028 s/m $^{1/3}$ and a uniform particle size of 40 mm were used. The mesh size used in this study is 70 m \times 10 m, which means 7 grid sizes in width and 3000 sizes in length. The time step used in this study is 0.2 second. The initial bed is uniformly flat for transverse direction without any perturbation, but, random perturbation is added to the transverse profile of upstream discharge to obtain a trigger for alternate bar formation and development in entire calculation time.

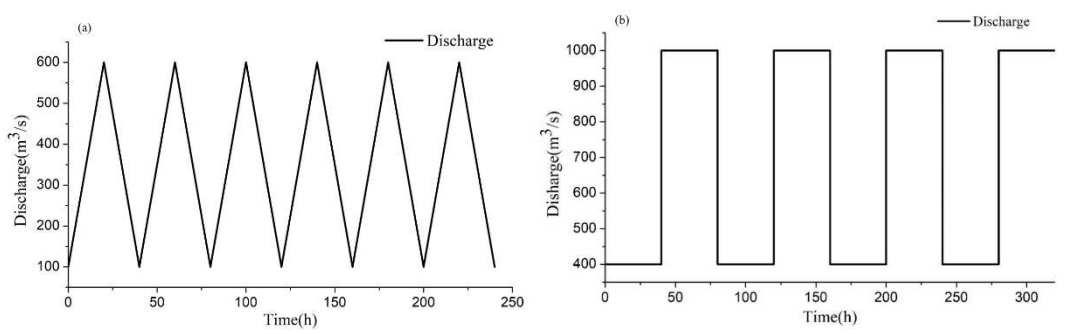


Figure 1 Hydrograph condition (a) Triangle cycle (b) Rectangular cycle

Figures 1 shows repeated hydrographs used in the calculation. As an example, Figure 1 (a) shows the discharge linearly increased from 100 to 600 m³/s within 20 h and subsequently decreased from 600 to 100 m³/s linearly in 20 h, forming a 40 h cycle. Six hydrographs are shown here as an example. In the calculation, 50 hydrographs were obtained. The sediment feed rate is the sediment transport capacity of this modeled river, and the supply rate depends on the hydrograph. As the feed rate is equivalent to the transport capacity, the bed elevation at the upstream end does not change over time under this condition.

Meanwhile, to test the influence of different discharges on the alternate bars, the following discharge processes are used with either fixed maximum discharge or fixed minimum discharge, giving a similar hydrograph as Figure 1 (a):

	Discharge (m ³ /s)					
Fixed maximum	100-700	200-700	300-700			
discharge of 700 m ³ /s						
Fixed minimum	400-600	400-700	400-800	400-900	400-1000	
discharge of 400 m ³ /s						

Table 1. Different discharge processes to test the morphodynamics of alternate bars

For each case, different hydrograph cycles of 10, 20, 40 and 80 hours are also tested for sensitivity analysis. The lowest discharge of 400 m³/s resulted in a fully transported condition of alternate bars, while the bars remained submerged and actively moved downstream. The highest discharge of 1000 m³/s can be determined by the upper transition limit between alternate bar formation and a no-bar condition based on the linear stability analysis. For the fixed maximum discharge cases, the purpose is to test the behavior of alternate bars when the discharge variation is around the critical value of 400 m³/s. For the fixed minimum discharge cases, the purpose is intended to make the migration of alternate bars active throughout the

computation. To observe the morphodynamic response of alternate bars more clearly, we performed a numerical simulation of alternate bars with an abrupt discharge change of 400–1000 m³/s as shown in Figure 1(b). The purpose of this case is to study the response time of alternate bars when the discharge rate changes. Low (or high) steady discharge first develops migrating alternate bars in a dynamic equilibrium state, and the abrupt change of discharge reshapes the bars to form another dynamic equilibrium state according to the high (or low) steady discharge.

In addition to the unsteady discharge case, we also performed calculation of steady water discharges at 400, 500, 600, 700, 800, 900, and 1000 m³/s. These discharges were set to be in the range of unsteady cases.

3. Results

3.1 Morphodynamic equilibrium and FFT analysis

Morphodynamic equilibrium is that alternate bars under a specific combination of discharge variation and hydrograph cycle reached an equilibrium state, that is, the wavelength and migration period of alternate bars remained constant, and the migration period was the same as the hydrograph cycle. This might be a unique morphodynamic feature of alternate bars under unsteady conditions because the steady discharge counterparts demonstrated a dynamic equilibrium state with slightly time-dependent features of the wavelength and migration period but did not exhibit non-time-dependent features. When morphodynamic equilibrium was reached, the hydrograph cycle was the dominant factor for alternate bar characteristics. If this morphodynamic state was achieved, the wavelength of alternate bars increased with the hydrograph cycle, and the migration period was always identical to the hydrograph cycle.

Here, we introduce FFT analysis as a treatment to for alternate bars morphodynamic equilibrium, by dealing with the elevation variation at one position with respect to time, the difference of alternate bars can be easily obtained. Figure 2 shows whether alternate bars in is in morphodynamic equilibrium state or not. Figure 2(a) indicate that the size and length of alternate bars are not the same, while Figure 2(b) shows a morphodynamic equilibrium state.

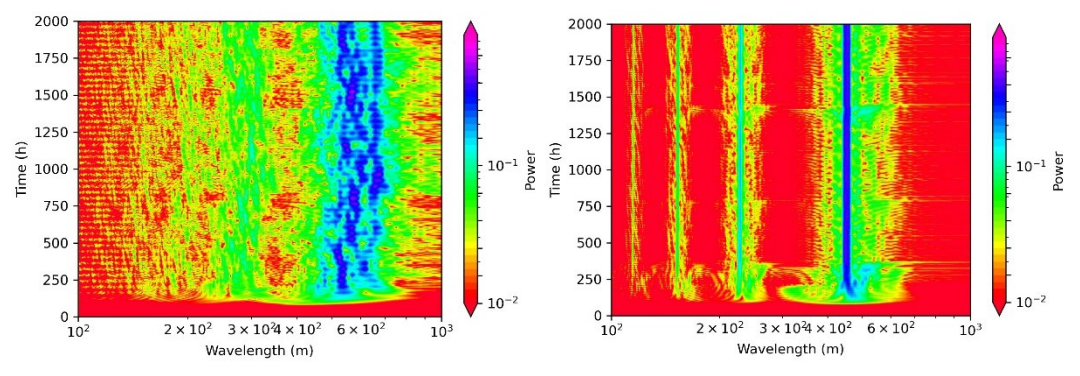


Figure 2 (Color) FFT analysis of wavelengths on (a) non-morphodynamic equilibrium state (b) morphodynamic equilibrium state

3.2 The conditions and criteria for the formation of morphodynamic equilibrium state

We imposed a repeated, identical, simple triangle-shape hydrograph for this alternate bar calculation, such that properties of the hydrograph, i.e., cycle and discharge range, might control this morphodynamic equilibrium state. Alternate bars showed unconventional

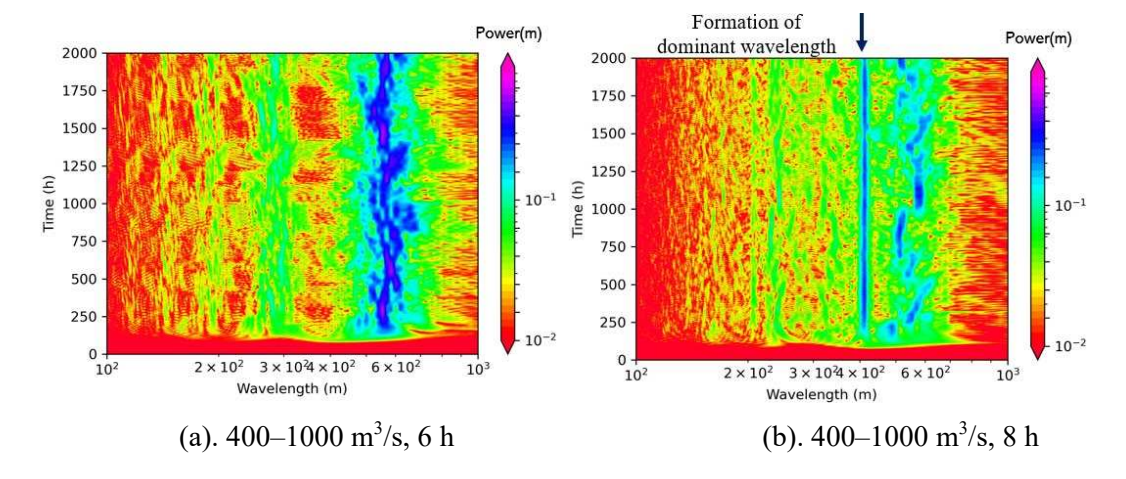
characteristics such as constant wavelength and migration periods after reaching morphodynamic equilibrium.

The occurrence of morphodynamic equilibrium caused by different unsteady discharge condition is summarized in Table 2, where the existence of the morphodynamics equilibrium is marked with a circle and the corresponding constant wavelength. In each case wherein the equilibrium state is achieved, the alternate bars have a unique constant wavelength, and their migration periods are equal to the hydrograph cycle. However, almost all the unsteady flow cases with a hydrograph cycle of 20 h can reach morphodynamic equilibrium. Furthermore, certain hydrograph cycles can also facilitate the alternate bars in reaching an equilibrium state.

Table 2. Hydrograph features for sensitivity analysis and existence of morphodynamic equilibrium that is indicated by open circles in this table, and equilibrium wavelength of alternate bars.

Discharge (m ³ /s)		Hydrograph cycle (hours)					
Min.	Max.	10	20	40	80		
100	600			○(550 m)	○(620 m)		
100			O(480 m)				
200	700		○(520 m)				
300			○(560 m)				
400	600		○(570 m)				
	700		○(590 m)				
	800		O(610 m)				
	900		O(640 m)				
	1000	○(457 m)	O(678 m)				

As the hydrograph cycles of 10 and 20 h provide the equilibrium state for a discharge variation of 400–1000 m³/s, cycle around 10 and 20 h was selected, that is, 6, 8, 12, 14, 16, 18, 25, and 30 h hydrograph cycles were used.



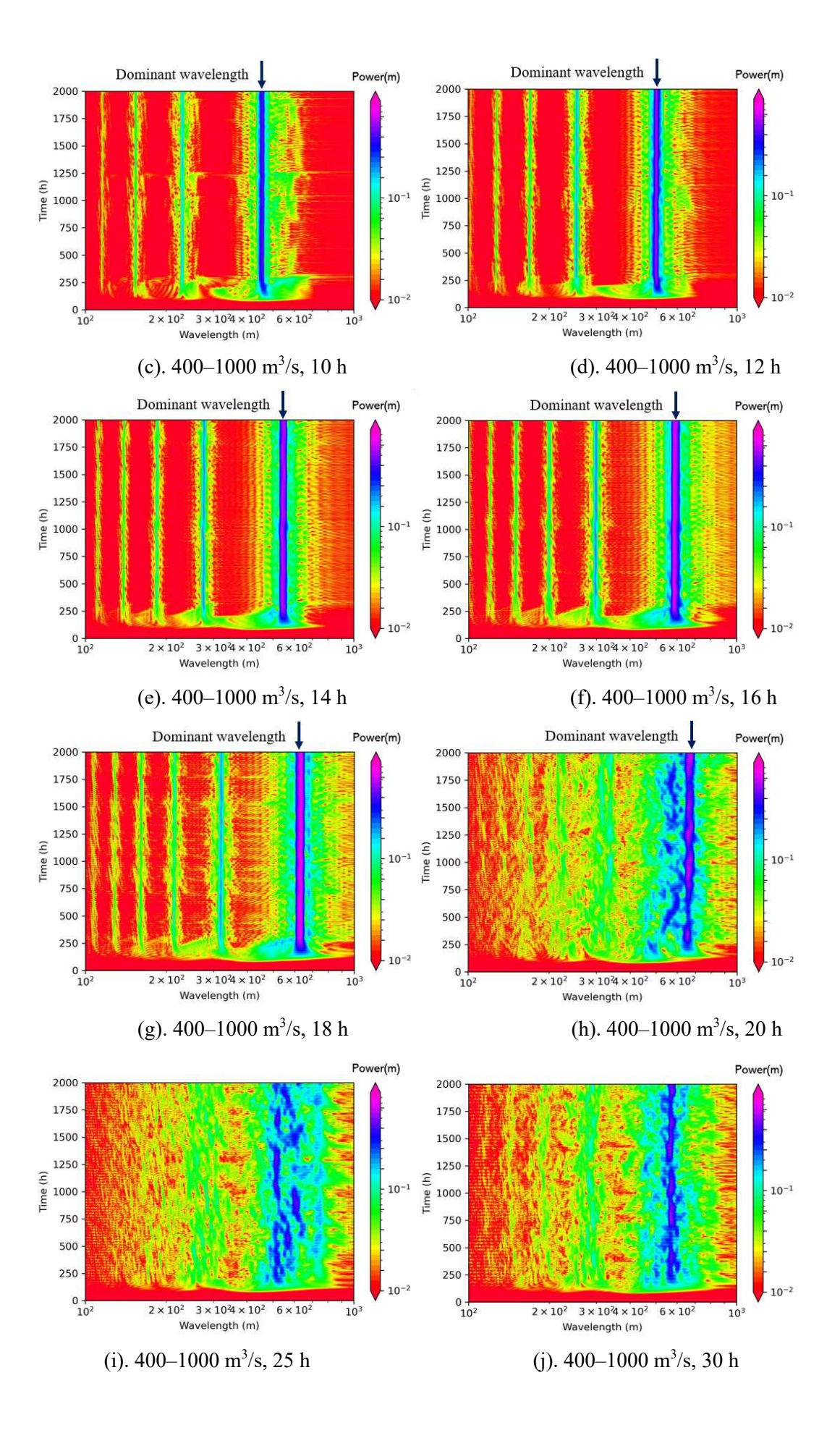


Figure 3 (a)–(j) (Color) FFT analysis of wavelengths in cases 400–1000 m³/s, cycles of 6, 8, 10, 12, 14, 16, 18, 20, 25, and 30 h.

Figure 3 shows the results of FFT analysis of these cases, showing that the hydrograph cycle that is in the range between 10 and 20 h provides an equilibrium state. Under this equilibrium state, the dominant wavelength caused by the 10, 12, 14, 16, 18, and 20 h hydrograph cycles are 457, 500, 539, 584, 637, and 678 m respectively, and the migration periods of these cases are identical to their hydrograph cycles. These results suggest that the hydrograph cycle is a dominant factor in determining the morphology of migrating alternate bars, that is, increasing the hydrograph cycle causes a longer wavelength and migration period. Conversely, the other cases show time-dependent morphodynamic features, i.e., dominant wavelength and migration period are highly variable with time.

3.3 Morphodynamics response of alternate bars under abrupt discharge change

The adjustment of bar shape is directly affected by the sediment transport rate q_b , which is further decided by the Shield number τ^* . Among the cases of 400-1000 m³/s, the difference of Shield number τ^* is decided by the flow velocity V and water depth h since all the conditions except hydrograph cycles are the same. Under a regular unsteady flow condition, V and h are able to change regularly, and further form the cyclic change of Shield number τ^* and sediment transport rate q_b . However, the change of sediment discharge will also cause topographic changes and in turn affect local water depth and velocity. Certainly, the formation of this reaction requires a certain time to accumulate and will not take effect immediately, which might be the reason why morphodynamics equilibrium state have time limits. To explore further, we performed a numerical simulation of alternate bars with an abrupt discharge change as it is introduced in the method section. The adjustment timescale of bar shape due to the discharge change might be an important factor in understanding the relation between hydrodynamic and morphodynamic timescales.

Figure 4 shows the time-space change of elevation variation at the right bank as we showed in Figure 1(b). In addition, Figure 5 demonstrates the temporal change of the elevation variation at the right bank within a certain time, when the discharge is abruptly decreased from 1000 m³/s to 400 m³/s and increased from 400 m³/s to 1000 m³/s, respectively. In the decreasing discharge process (the discharge drops at 800 h), elevation variation between 797–820 h is shown in Figure 5 (a). In the increasing discharge process (the discharge abruptly increase at 840 h), elevation variation from 837–860 h is shown in Figure 5 (b).

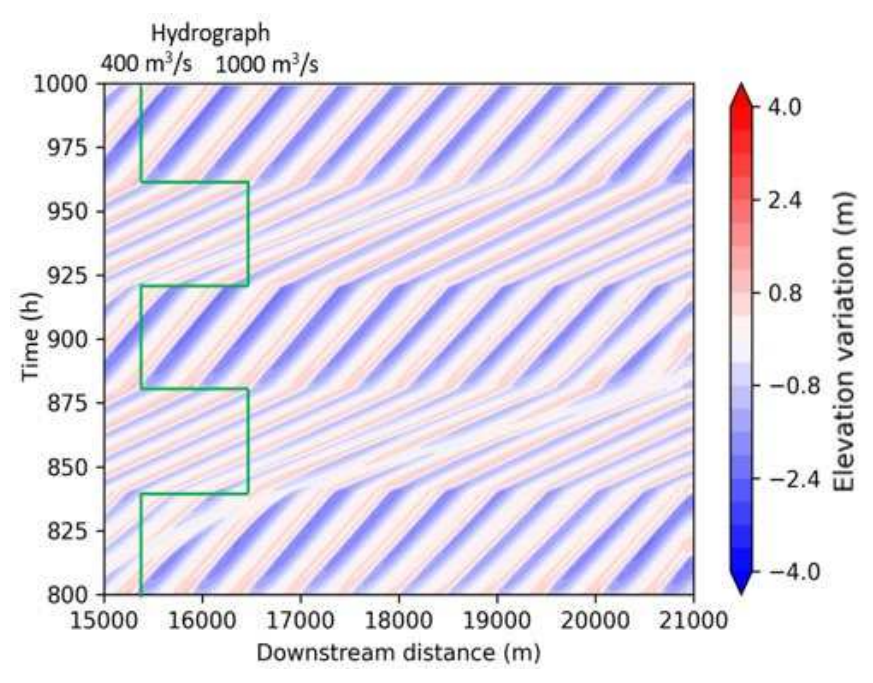


Figure 4 (Color) Elevation variation at the right bank along time and downstream distance with the hydrograph.

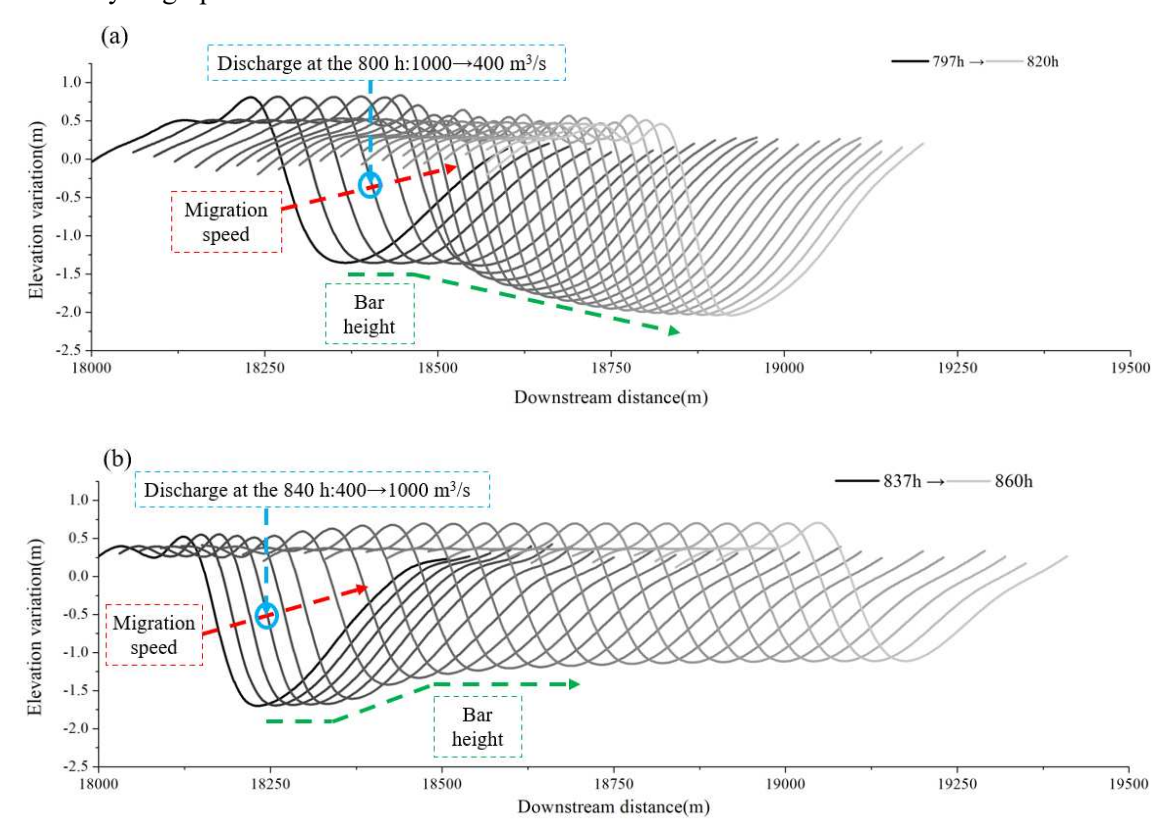


Figure 5 (Color) Elevation variation of the right bank when discharge (a) decreases from $1000 \text{ m}^3/\text{s}$ to $400 \text{ m}^3/\text{s}$; (b) increases from $400 \text{ m}^3/\text{s}$ to $1000 \text{ m}^3/\text{s}$.

Figure 4 shows that the migration speed of alternate bars changes rapidly as the discharge abruptly changes. The same phenomenon can be observed in Figure 5, which has been marked with a red dotted arrow. The migration speed of the alternate bar tops changed rapidly within

3–4 h after the discharge changed. Figure 5 (a) shows a discharge reduction from 1000 m³/s to 400 m³/s, and a subsequent decrease in the bottom of the alternate bars indicated by the green dotted arrow, which represents an increasing bar height. However, unlike the rapid change in the migration speed, the change in bar height is a longer process. In Figure 5 (a), the decrease in the elevation of the bottom point lasts for 20 h, and still maintains a decreasing trend. Figure 5 (b) shows a discharge increase from 400 m³/s to 1000 m³/s, and a subsequent increase in the bottom of the alternate bars indicated by the green dotted arrow, which represents a decreasing bar height. Similarly, the migration speed changes rapidly, and the change in bar height is a long-term process. However, in Figure 5 (b), the bar height appears to reach an equilibrium state after 6–8 h. The elevation variation due to discharge increase is much faster than that when the discharge decreases from 1000 m³/s to 400 m³/s.

The short response time of migration speed indicates simultaneous change of migration speed and discharge. In our study, the discharge variation is linear and smooth, so that the migration speed changes without any lag, contributing to the migration pattern shown in Figure 1(b). The migration speed of all alternate bars changes with discharge and eventually maintains an approximate constant of the average velocity. Contrastingly, the longer response time of the bar height suggests that, for different discharge changes, different time periods are required for the alternate bars to reach the corresponding bar height and wavelength. For lower discharge rates, a much longer time is required for alternate bars to reach equilibrium state because of low sediment transport capacity. The height of alternate bars reaches an equilibrium state quicker for higher discharge rates because the sediment transport capacity is high.

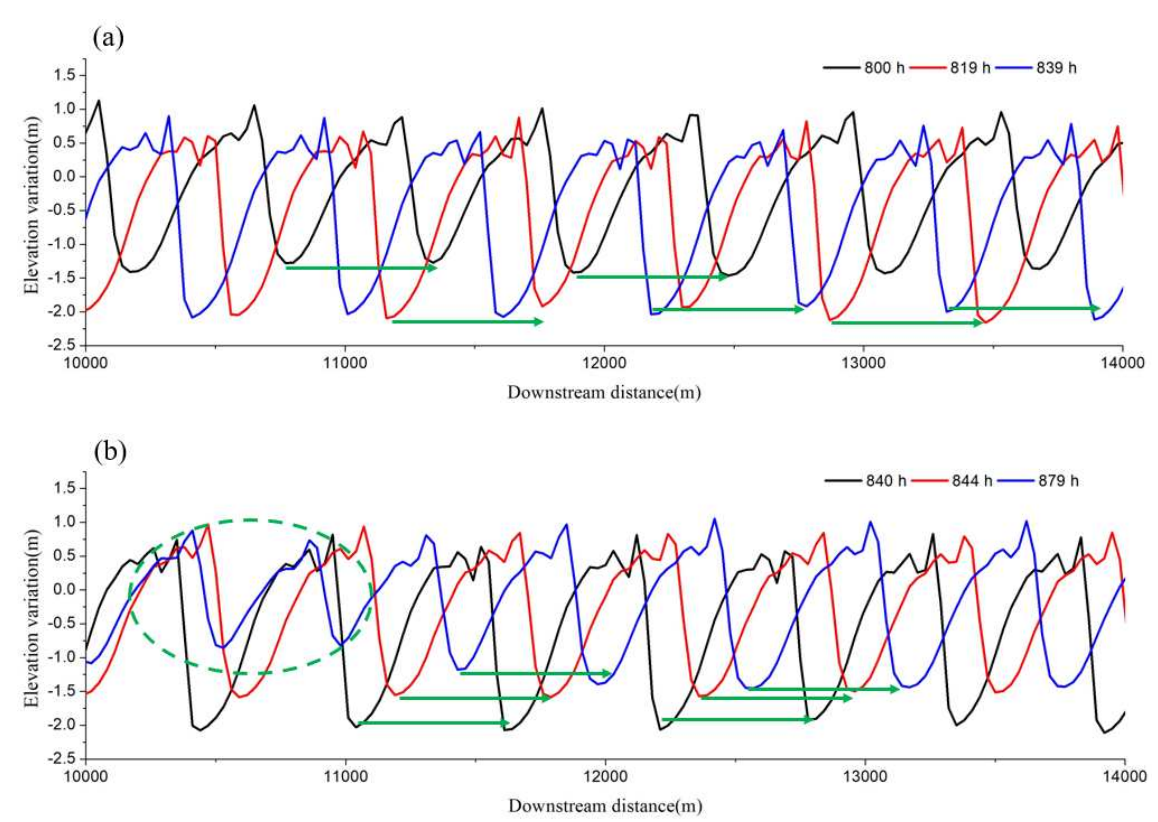


Figure 6 (a) (Color) Elevation variation of the right bank at 800, 819, and 839 h when discharge drops from 1000 m³/s to 400 m³/s. (b) (Color) Elevation variation of the right bank at the 800, 819, and 839 h when discharge increases from 400 m³/s to 1000 m³/s.

Figure 6 shows the response conditions of bar height and wavelength to a discharge change from 1000-400 m³/s and 400-1000 m³/s. The green arrow line represents a 570 m length and is used to measure the wavelength of the alternate bars. Figure 4 (a) shows that the wavelength of bars does not change during the discharge-dropping process. On the contrary, in the discharge-increasing process shown in Figure 6 (b), different wavelengths appear at 879 h, while the wavelengths at 840 h and 844 h remain at 570 m. Furthermore, the shape of alternate bars may also change, as depicted inside the green dotted circle. The results show that the wavelength of alternate remains stable in the discharge-dropping process as opposed to the increasing process. The wavelength remains the same in both processes until the bar height reaches equilibrium state. After the that, for the discharge-increasing process, the wavelength changes, as shown at 844 h and 879 h. This is because after the alternate bars reach a steady discharge pattern, it is much easier for the bar to change its wavelength. However, for the discharge-dropping process, the response time is much longer, the alternate bars cannot reach a steady discharge pattern, and the wavelength remains constant for a longer period. This difference in response time is caused by the sediment transport rate in lower and higher discharges, implying that the higher sediment transport rate makes the adjustment time for the discharge change faster.

According to the result, there are three response stages of the alternate bars to discharge change. First is the quick response of the migration speed, while bar height changes until the dynamics of alternate bars reach the equilibrium state under given steady discharge level. The required time for the alternate bars to reach a steady flow state is dependent on the discharge, ranging from 5 h (during 400–1000 m³/s) to more than 20 h (during 1000–400 m³/s). After the alternate bars reach the steady flow state, their wavelengths might change according to the alternate bar properties.

The hydrograph cycle that provides the morphodynamics equilibrium state might lie between the two-threshold response times that distinguish three response stages explained above. The hydrograph cycle should be long enough for the alternate bars to respond to discharge variation, but not too long to allow the alternate bars to reach the equilibrium bar height and begin to deform their wavelength as they do in steady flow conditions. If the hydrograph cycle is too short, the alternate bars can be unstable as the discharge variation of $400-1000 \, \mathrm{m}^3/\mathrm{s}$ with 6 h cycle case shows. If the hydrograph cycle is too long, the alternate bars have enough time to deform. In this case, the alternate bars have a chance to develop and become unstable or show cyclic behaviors like under steady discharge condition.

4. Conclusions

In this study, we numerically investigated the morphodynamic equilibrium of alternate bars, a morphodynamic state in which the wavelength of alternate bars increased with the hydrograph cycle, and the migration period was always identical to the hydrograph cycle. The hydrograph cycle that corresponds to this equilibrium state can be determined from the relation between hydrodynamic and bar growth timescales. Under a short hydrograph, the bar growth occurred much slower than the discharge changes, so that the bars cannot respond to the discharge variation. Meanwhile, the long hydrograph provided sufficient time for the

deformation and development of alternate bars, causing a significant change in bar characteristics (e.g., wavelength) within one hydrograph such as steady discharge condition. The hydrograph cycle that achieves this equilibrium state must be moderately long so that the timescale of the hydrograph is similar but slightly smaller than the bar growth timescale, but not too small to allow equilibrium bar behaviors caused by steady discharge conditions.

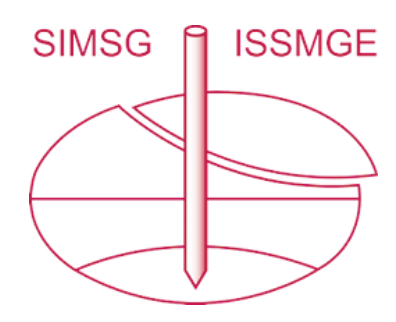
References:

- A. Crosato, A. Grissetti-Vázquez, F. Bregoli, et al, Adaptation of river channels to a wetter or drier climate: Insights from the Lower Pilcomayo River, South America, J. Journal of Hydrology, (2022), 128254. https://doi.org/10.1016/j.jhydrol.2022.128254.
- G. Duró, A. Crosato, P. Tassi, Numerical study on river bar response to spatial variations of channel width, J. Advances in Water Resources, (2016), 93: 21–38. https://doi.org/10.1016/j.advwatres.2015.10.003.
- F. Amoako Johnson, C.W. Hutton, Dependence on agriculture and ecosystem services for livelihood in Northeast India and Bhutan: vulnerability to climate change in the Tropical River Basins of the Upper Brahmaputra, J. Climatic Change, (2014), 127(1): 107–121. https://doi.org/10.1007/s10584-012-0573-7.
- M. Jaballah, B. Camenen, L. Pénard, et al, Alternate bar development in an alpine river following engineering works, J. Advances in Water Resources, (2015), 81: 103–113. https://doi.org/10.1016/j.advwatres.2015.03.003.
- Y. Fujita, Y. Muromoto, Studies on the process of development of alternate bars, J. Bulletin of the Disaster Prevention Research Institute, (1985), 35(3): 55–86.
- M. Colombini, G. Seminara, M. Tubino, Finite-amplitude alternate bars, J. Journal of Fluid Mechanics, (1987), 181: 213–232. https://doi.org/10.1017/s0022112087002064.
- T.E. Lisle, H. Ikeda, F. Iseya, Formation of stationary alternate bars in a steep channel with mixed size sediment: A flume experiment, J. Earth Surface Processes and Landforms, (1991), 16(5): 463 469. https://doi.org/10.1002/esp.3290160507.
- S. Ikeda, Prediction of alternate bar wavelength and height, J. Journal of Hydraulic Engineering, (1984), 110(4): 371–386. https://doi.org/10.1061/(asce)0733-9429(1984)110:4(371).
- A. Defina, Numerical experiments on bar growth, J. Water Resources Research, (2003), 39(4). https://doi.org/10.1029/2002wr001455.
- P.J. Whiting, W.E. Dietrich, Experimental constraints on bar migration through bends: Implications for meander wavelength selection, J. Water Resources Research, (1993), 29(4): 1091–1102. https://doi.org/10.1029/92wr02356.
- A. Crosato, F.B. Desta, J. Cornelisse, et al, Experimental and numerical findings on the long-term evolution of migrating alternate bars in alluvial channels, J. Water Resources Research, (2012), 48: W06524. https://doi.org/10.1029/2011wr011320.
- M. Tubino, Growth of alternate bars in unsteady flow, J. Water Resources Research, (1991), 27(1): 37–52. https://doi.org/10.1029/90wr01699.
- Y. Watanabe, M. Tubino, G. Zolezzi, et al, Behavior of alternate bars under unsteady flow conditions, C. 2nd IAHR Symposium On River, Coastal and Estuary Morphodynamics, Obihiro,

- Japan. Sapporo, Japan: Hokkaido Univ. Press, (2001): 673-682.
- N. Izumi, M. Takatsu, S. Kawamura, Effects of the variation of discharge on the growth of fluvial bars, Journal of Japan Society of Civil Engineers, Ser. A2 (Applied Mechanics), (2021), 77(2): I_451-456. https://doi.org/10.2208/jscejam.77.2_i_451.
- P. Hall, Alternating bar instabilities in unsteady channel flows over erodible beds, Journal of Fluid Mechanics, (2004), 499: 49–73. https://doi.org/10.1017/s0022112003006219.
- F. Visconti, C. Comporeale, L. Ridolfi, Role of discharge variability on pseudomeandering channel morphodynamics: Results from laboratory experiments, Journal of Geophysical Research, (2010), 115: F04042. https://doi.org/10.1029/2010jf001742.
- T. Iwasaki, Y. Shimizu, I. Kimura, Numerical simulation of bar and bank erosion in a vegetated floodplain: A case study in the Otofuke River, J. Advances in Water Resources, (2016), 93: 118–134. https://doi.org/10.1016/j.advwatres.2015.02.001.
- M. Carlin, M. Redolfi, M. Tubino, The long-term response of alternate bars to the hydrological regime, J. Water Resources Research, 2021, 57: e2020WR029314. https://doi.org/10.1029/2020wr029314.
- M, Church, S.P. Rice, Form and growth of bars in a wandering gravel-bed river, J. Earth Surface Processes and Landforms, (2009), 34(10): 1422-1432. https://doi.org/10.1002/esp.1831
- P.A. Nelson, J.A. Morgan, Flume experiments on flow and sediment supply controls on gravel bedform dynamics, J. Geomorphology, (2018), 323: 98–105. https://doi.org/10.1016/j.geomorph.2018.09.011.
- M. Colombini, A. Stocchino, Three-dimensional river bed forms, J. Journal of Fluid Mechanics, (2012), 695: 63–80. https://doi.org/10.1017/jfm.2011.556.
- D.J. Furbish, Irregular bed forms in steep, rough channels: 1. Stability analysis, J. Water Resources Research, (1998), 34: 3635–3648. https://doi.org/10.1029/98wr02339.
- Y. Shimizu, S. Giri, S. Yamaguchi, et al, Numerical simulation of dune-flat bed transition and stage-discharge relationship with hysteresis effect, J. Water Resources Research, (2009), 45(4): W04429. https://doi.org/10.1029/2008wr006830.
- Y. Shimizu, H. Takebayashi, T. Inoue, et al, iRIC-Software: Nays2DH solver manual. (2014), Available online: https://i-ric.org/en/ (accessed on 25 October 2021).
- J.M. Nelson, Y. Shimizu, T. Abe, et al, The international river interface cooperative: Public domain flow and morphodynamics software for education and applications, J. Advances in Water Resources, (2016), 93: 62–74. https://doi.org/10.1016/j.advwatres.2015.09.017.
- T. Kang, I. Kimura, Y. Shimizu, Numerical simulation of large wood deposition patterns and responses of bed morphology in a braided river using large wood dynamics model, J. Earth Surface Processes and Landforms, (2020), 45(4): 962–977. https://doi.org/10.1002/esp.4789.
- P. Rahman, M.S. Ali, Change in transverse slope of water surface at river bend: A numerical study, J. Journal of Engineering Science, (2021), 12(2): 93–101. https://doi.org/10.3329/jes.v12i2.54634.
- A.D. Tamminga, B.C. Eaton, C.H. Hugenholtz, UAS based remote sensing of fluvial change following an extreme flood event, J. Earth Surface Processes and Landforms, (2015), 40(11): 1464 1476. https://doi.org/10.1002/esp.3728.
- H. Dai, T. Iwasaki, Y. Shimizu, Effect of sediment supply on morphodynamics of free alternate bars: Insights from hydrograph boundary layer, J. Water, (2021), 13(23): 3437. https://doi.org/10.3390/w13233437.

- L.G. MacKenzie, B.C. Eaton, Large grains matter: contrasting bed stability and morphodynamics during two nearly identical experiments, J. Earth Surface Processes and Landforms, (2017), 42(8): 1287–1295. https://doi.org/10.1002/esp.4122.
- T. Kyuka, K. Okabe, Y. Shimizu, et al, Dominating factors influencing rapid meander shift and levee breaches caused by a record-breaking flood in the Otofuke River, Japan, J. Journal of Hydro-environment Research, (2020), 31: 76–89. https://doi.org/10.1016/j.jher.2020.05.003.
- T. Nagata, Y. Watanabe, H. Yasuda, A. Ito, Development of a meandering channel caused by the planform shape of the river bank, J. Earth Surface Dynamics, (2014), 2: 255–270. https://doi.org/10.5194/esurf-2-255-2014.
- A. Grossmann, J. Morlet, Decomposition of hardy functions into square integrable wavelets of constant shape, J. SIAM Journal on Mathematical Analysis, (1984), 15(4): 723–736. https://doi.org/10.1137/0515056.
- Y.A. Cataño-Lopera, J.D. Abad, M.H. García, Characterization of bedform morphology generated under combined flows and currents using wavelet analysis, J. Ocean Engineering, (2009), 36(9–10): 617–632. https://doi.org/10.1016/j.oceaneng.2009.01.014.
- M. Mahdade, N. Le Moine, R. Moussa, et al, Automatic identification of alternating morphological units in river channels using wavelet analysis and ridge extraction, J. Hydrology and Earth System Sciences, (2020), 24(7): 3513–3537. https://doi.org/10.5194/hess-24-3513-2020.
- M. Kuroki, T. Kishi, Regime criteria on bars and braids in alluvial straight channels, J. Proc. of JSCE, (1984), 342: 87–96. (in Japanese) https://doi.org/10.2208/jscej1969.1984.342 87.

INTERNATIONAL SOCIETY FOR SOIL MECHANICS AND GEOTECHNICAL ENGINEERING



This paper was downloaded from the Online Library of the International Society for Soil Mechanics and Geotechnical Engineering (ISSMGE). The library is available here:

https://www.issmge.org/publications/online-library

This is an open-access database that archives thousands of papers published under the Auspices of the ISSMGE and maintained by the Innovation and Development Committee of ISSMGE.

The paper was published in the proceedings of the 12th International Conference on Scour and Erosion and was edited by Shinji Sassa as the Chair of the TC213 on Scour and Erosion. The conference was held in Chongqing, China from November 4th to November 7st 2025.